# IMPACT OF NOISE ON THE POLARIMETRIC IMAGING BASED SHAPE RECOVERY OF TRANSPARENT OBJECTS

*Romain ROUX, Jihad ZALLAT, Alex LALLEMENT, Ernest HIRSCH*

Laboratoire des Sciences de l'Image, de l'Informatique et de la Télédétection (UMR ULP-CNRS 7005),
Université Louis Pasteur – Strasbourg I,
Parc d'innovation, Boulevard Sébastien Brant, BP 10413, F-67412 Illkirch-Cedex, France
Phone : +33 3 90 24 45 29, fax : +33 3 90 24 45 31, email : roux@lsiit.u-strasbg.fr

## ABSTRACT

*In the field of computer vision, specifically for applications aiming at the accurate 3D reconstruction of either natural or hand-made objects, only a few methods are able to recover the shape of transparent objects. Among these, polarimetric imagery has already proved its ability to deal with such objects. In this paper, after a short presentation of the theoretical background leading to the proposed approach for recovering the shape of transparent surfaces, various processing techniques for polarimetric data are described. In particular and firstly, the advantages implied by the use of measures relying on the full so-called Stokes vector are highlighted. Secondly, the method used for denoising multi-channel polarimetric image data, in order to improve the following surface recovery process, is introduced. Lastly, the efficiency of the suggested method is demonstrated through experimental results obtained using simulated surface data..*

## 1. BACKGROUND

For computer vision based applications, such as the quantitative reconstruction of machined parts in view of quality control, it is necessary to make available efficient tools for the computation of their 3D descriptions out of the image contents. Such workpieces more and more include transparent or semi-transparent surface patches. Thus, 3D information cannot be obtained by imaging the objects solely using a standard CCD sensor. But only very few methods devised for shape recovery can deal with (semi-)transparent surfaces. This stems mainly from the fact that it is nearly impossible to determine in standard grey-level images, which part of the intensity measured originates from the inner of the transparent object and, consequently, to take this contibution away from the acquired data values. Using a polarimetric imaging device enables to determine these intensity contributions, these light intensity components being nearly unpolarized. After having removed the undesirable intensity contributions, the 3D coordinates of selected image features can be derived using triangulation methods based on a pair of polarimetric images.
We present in the second section Fresnel's reflection model and how it is linked to the polarization state of light, when light is reflected by a transparent surface. In the third part, we describe the so-called "Scatter Plot Method", which allows to filter out the noise in polarimetric images and, thus, to improve the accuracy of the following reconstruction step. Simulated results are shown in the fourth section, and the last section provides a short outlook. A brief presentation of the state-of-the-art is given hereafter.
Koshikawa, in [5], assuming that the surface reflectance is totally specular, shows that, with circularly polarized incident light and some *a priori* knowledge about the nature of the material (refractive index ; behaviour of selected parameters measured using a polarizer positioned in front of a camera), one can determine the orientation of the outer surface of an object. Likewise, Wolff, in [11-12], assuming totally unpolarized incident light, proves that, using two cameras fitted with polarizers, enables to recover the orientation of a glossy surface. But his method is restricted to the recovery of plane surfaces. This is due to the fact that registering the two required views cannot currently be achieved when imaging transparent objects. For plane surfaces, he determines the orientation of the two planes of incidence and their intersection, which in turn yields the direction of the normal to the imaged 3D plane.

## 2. STOKES VECTOR OF A SPECULAR REFLECTION

This section provides the necessary theoretical background.
According to Fresnel's reflection model shown in figure 1, the reflection components $R_\perp$ and $R_{II}$ are directly linked to the angle of incidence of the light $\theta_i$ and the refraction index *n:*

$$R_\perp^2 = \frac{\sin(\theta_i - \theta_t)^2}{\sin(\theta_i + \theta_t)^2} \quad (1)$$

$$R_\parallel^2 = \frac{\tan(\theta_i - \theta_t)^2}{\tan(\theta_i + \theta_t)^2} \quad (2)$$

The transmission angle $\theta_t$ is given by Snell's well-known relation. The degree of polarization (DOP) $\rho$ can then be expressed using equations (1) and (2) for $R_\perp$ and $R_{II}$ respectively:

$$\rho = \frac{R_\perp^2 - R_\parallel^2}{R_\perp^2 + R_\parallel^2} \quad (3)$$

which leads to :

$$\rho = \frac{2\sin\theta_i \tan\theta_i \sqrt{n^2 - \sin^2\theta_i}}{n^2 - \sin^2\theta_i + \sin^2\theta_i \tan^2\theta_i} \quad (4)$$

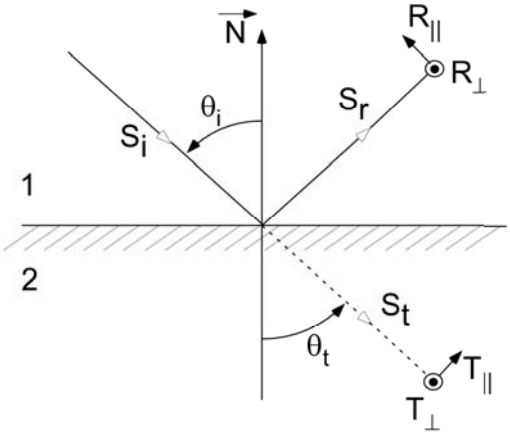


Figure 1 – Fresnel's model of reflection

Knowing all the DOP values over a given surface patch, equation (4) enables to determine the angle of incidence of the light for each pixel position and, then, the zenith of the corresponding surface point. However, equation (4) is not bijective, as illustrated in figure 2. The limit for a surjective behaviour is observed at the Brewster angle $\theta_B$. At this particular angle, $\rho = 1$.

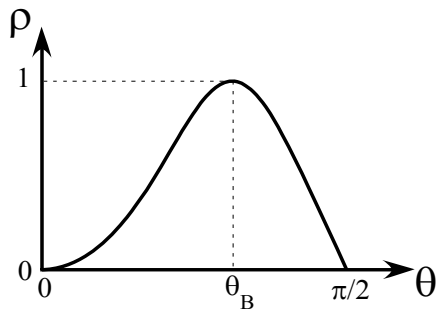


Figure 2 – Degree of polarization versus the angle of incidence

To solve for this ambiguity, Miyazaki and *al.* suggest an approach allowing deciding if $\theta_i < \theta_B$ or not for each pixel. In [8], they firstly used two distinct sets of measurements of the DOP, one obtained in the visible spectrum of wavelengths, the other in the infra-red domain. As a matter of fact, the DOP obtained in the infra-red domain is bijective, but measurements are usually too noisy and only allow a comparison of zenith values, computed in the visible spectrum, with $\theta_B$. Secondly, in [9], they apply a segmentation-based method, which enables to remove the ambiguity for some areas of the object surface. By tilting these aeras, and calculating the variation of the DOP for the positions of these areas in the two images, they solve for the ambiguity for the whole imaged surface. Lastly, they use an iterative method based on Muller calculus and an inverse polarization ray-tracing procedure. Comparing iteratively the measured polarization images with simulated ones generated using the results from the previous iteration steps, the approach converges to a satisfactory reconstructed shape. In this contribution, we suggest a method based on the measure of the full Stokes vector, which enables to derive the desired shape, under natural illumination, without applying an iterative scheme and *a priori* knowledge of the refraction index. The approach is further combined with a filtering step based on the Scatter Plot Method [1], allowing this way to obtain more effective results.

As it is well known, a 4x1 Stokes vector represents the polarization state of light. The 4x4 so-called Mueller matrix is the associated operator, which describes how the polarization state of light is changed, when light interacts with the surface of an object. Given the Mueller matrix $M$ of an optical system and the Stokes vector $S$ of the incident light, one gets directly the Stokes vector $S'$ of the reflected light, according to equation (5) :

$$S' = M.S = M.\begin{pmatrix} S_0 \\ S_1 \\ S_2 \\ S_3 \end{pmatrix} \quad (5)$$

After reflection of the light on the surface, according to Fresnel's model, the Mueller matrix $M$ can be expressed as follows:

$$M_r = \frac{1}{2}\begin{pmatrix} R_\perp^2 + R_\parallel^2 & R_\perp^2 - R_\parallel^2 & 0 & 0 \\ R_\perp^2 - R_\parallel^2 & R_\perp^2 + R_\parallel^2 & 0 & 0 \\ 0 & 0 & 2R_\perp R_\parallel & 0 \\ 0 & 0 & 0 & 2R_\perp R_\parallel \end{pmatrix} \quad (6)$$

Furthermore, reflection introduces some delay between the parallel and orthogonal components of the wave, which can be modelled by the following Mueller matrix:

$$L(\varphi) = \begin{pmatrix} 1 & 0 & 0 & 0 \\ 0 & 1 & 0 & 0 \\ 0 & 0 & \cos(\varphi) & \sin(\varphi) \\ 0 & 0 & -\sin(\varphi) & \cos(\varphi) \end{pmatrix} \quad (7)$$

Finally, after rotation of the whole Mueller matrix in order to align it with the plane of incidence, one obtains:

$$M = R(-\alpha).M_r.L(\varphi).R(\alpha) \quad (8)$$

As shown on figure 3, the angle α represents the direction of the plane of incidence. This angle corresponds also to the azimuth of the surface normal. As we are working under natural ambient illumination, which can be considered totally unpolarized, the corresponding Stokes vector can be written as:

$$S' = M.S = \frac{1}{2}\begin{pmatrix} R_\perp^2 + R_\parallel^2 \\ (R_\perp^2 + R_\parallel^2)\sin(2\alpha) \\ (R_\perp^2 + R_\parallel^2)\cos(2\alpha) \\ 0 \end{pmatrix} \quad (9)$$

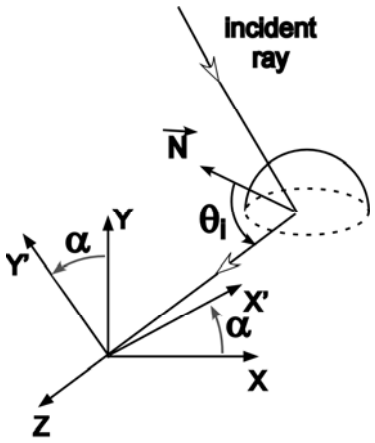

Figure 3 – reflection parameterization

Thus, measuring the Stokes vector of the reflected light enables to compute:

$R_{\parallel}^2$ , $R_{\perp}^2$ and $2\alpha$ .

Hence, according to equations (1) and (2), we can calculate the angle of incidence $\alpha$, which corresponds, as shown on figure 4, to the zenith of the surface normal (*cf.* also figure 3). The refractive index $n$ is computed using image data according to:

$$R_{\parallel} = 0 \tag{10}$$

This computation is carried out at the Brewster angle $\theta_B$ given by :

$$\theta_B = \tan^{-1} n \tag{11}$$

As a result, at this angle, one can write:

$$R_{\perp}^2 = \left( \frac{n^2 - 1}{n^2 + 1} \right)^2 \tag{12}$$

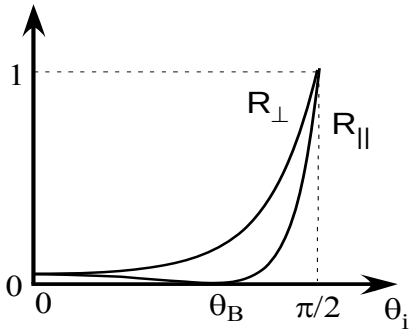

Figure 4 – Fresnel's reflection components

Equation (12) is easily solved, assuming that:

$$n \geq 1 \tag{13}$$

Lastly, the azimuth is still only known with the following ambiguity of $\pm\pi$ :

$$\alpha_{computed} = \alpha_{true} \pm \pi \tag{14}$$

In order to remove this ambiguity, we shall assume that the surface is convex. Knowledge of the azimuth is then "propagated" from the occluding boundary of the analysed surface, where this quantity is known without ambiguity, to the inner of the surface. At the end of this step, we obtain the maps of the zenith and azimuth values over the whole surface. In order to reconstruct the shape of the object, we make use of either the shapelet-based method proposed by Kovesi [7], the multi-resolution relaxation method, or the approach developed by Wei and Klette [10]. The shapelet method has however a strong advantage over the other two. It allows reconstructing the shape, up to a convex/concave shape ambiguity, without having to refine further the azimuth data in order to remove a remaining ambiguity. Using a Fourier Transform makes the Wei and Klette method very fast, in comparison to the iterative relaxation method proposed by Horn [3]. Their method is however less efficient. Results are to be discussed in section 4.

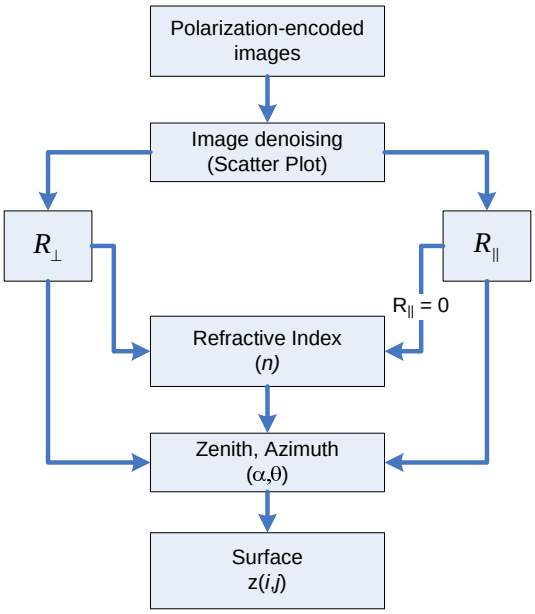

Figure 5 – Overview of the method

## 3. DENOISING OF POLARIMETRIC IMAGES

The measured data contains noise originating from various sources, such as misalignment of the optical elements of the acquisition system, small deviations in their (calibrated) parameter values and errors inherent to the CCD sensor. As can be expected, this noise limits the efficiency and accuracy of the reconstruction process. In order to remove as much as possible the noise, we make use of the Scatter Plot Method described by Aiazzi *et al.* in [1]. in [1]. For that purpose, the mean $\mu(i, j)$ and standard deviation (STD) $\sigma(i, j)$ are computed over the whole image applying a sliding window of size $m \times m$ pixels and according to the equations below:

$$\begin{aligned} \mu(i,j) &= \frac{1}{m^2 - 1} \sum_{k=-m/2,m/2} \sum_{l=-m/2,m/2} g(i-l, j-k) \\ \sigma(i,j) &= \frac{1}{m^2 - 1} \sum_{k=-m/2,m/2} \sum_{l=-m/2,m/2} \left[ g(i-l, j-k) - \mu \right]^2 \end{aligned} \tag{15}$$

Then, the method exploits the plot of $\sigma$ versus $\mu$. After tiling the domain $(\sigma, \mu)$ with a fixed number of blocks, the authors determine those blocks, which contain the greatest number of pixels. These blocks, and the corresponding pixels selected this way, can be associated with the homogeneous areas in the image. For these pixels, an estimate of the noise level $\hat{n}$, can be obtained according to:

$$\hat{n}(i,j) = \sqrt{\frac{(2m+1)^2}{(2m+1)^2 - 1}}\left[g(i,j) - \mu(i,j)\right] \qquad (16)$$

In equations (15) and (16) above, $g(i,j)$ stands for the acquired image and $\mu(i,j)$ for the map of means computed during the first step of the denoising process.
In this way, assuming that the noise is additive, we obtain at the end of the denoising process an estimate of the noise-free image corresponding to the acquired image.

## 4. RESULTS

In order to test the efficiency of the denoising step, we have generated simulated polarimetric images, to which we have added varying amounts of Gaussian noise. The shape of the imaged objects has, then, be reconstructed, with and without filtering the images using the Scatter Plot Method described in section 3. The experimental procedure is summarized in figure 5. For our experiments, we have made use of a surface parameterized as follows:

$$z(x,y) = abs\left(p.\sin\left(\frac{\pi x}{p}\right).\sin\left(\frac{\pi y}{p}\right)\right) \qquad (17)$$

where *p* corresponds to the length, as well as to the width of the surface. The polarimetric images are firstly computed, *i.e.* the images of each Stokes parameter are calculated. After having added Gaussian noise, the latter is removed applying the Scatter Plot Method. Lastly, we proceed with the reconstruction step. The various steps of the experimental procedure, for the third parameter of the Stokes vector, are illustrated on figure 6. On figures 7 and 8, the efficiency of the filtering method is demonstrated on image data with noise levels of increasing STD value. As expected, reconstructions based on filtered data are less dependent on the noise level. The Scatter Plot Method shows, thus, a real efficiency in order to remove noise in polarimetric images. In our simulation, the signal-to-noise ratio is of the order of 0dB for a noise with STD = 0.02. The error in the determination of the refractive index *n* out of images with a signal-to-noise ratio of 0dB is less than 1%. Indeed, our method yields *n* = 1.5124 instead of *n* = 1.5. Regarding the assessment of the reconstructions obtained, the Shapelet-based approach provides more accurate and robust results than those obtained with the Wei and Klette method. However, one must keep in mind that the step applied to the azimuth data in order to remove the ambiguity is very sensitive to noise. Experimentally, the shapelet method appears to be less efficient, when applied to azimuth data without ambiguity.

## 5. CONCLUSION AND FUTURE WORK

In this contribution, we have described an approach for recovering the shape of transparent objects using a full Stokes polarimeter. The method allows to circumvent operational complexity usually associated with other techniques, as described, for example, in [5,6,8,9,11], and related to object tilting, the use of additional measurements in the infrared domain, and the preliminary segmentation of the images. We have shown that Stokes imaging simplifies both the acquisition step and the determination of the coordinates of the surface normals. In order to improve the reliability of the reconstruction, we made use of the Scatter Plot Method, which proved its ability to efficiently filter out the noise in polarimetric images. Due to the remaining ambiguity of $\pi$ in the azimuth data (*cf.* Equation (14)), reconstructions are presently strictly limited to convex objects. To overcome this restriction, future work will extend the described approach to the use of stereovision.

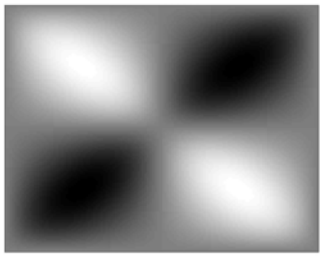

(a)

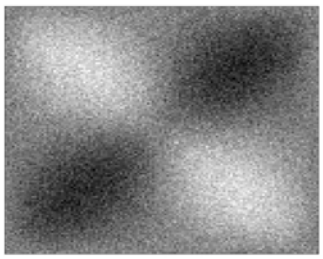

(b)

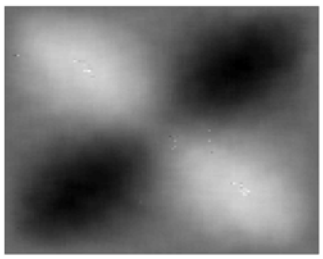

(c)

Figure 6 – The S3 Stokes parameter images. (a) is the noise free simulated image, (b) same as (a) with a white Gaussian noise where SNR = 0dB and (c) is the filtered one.

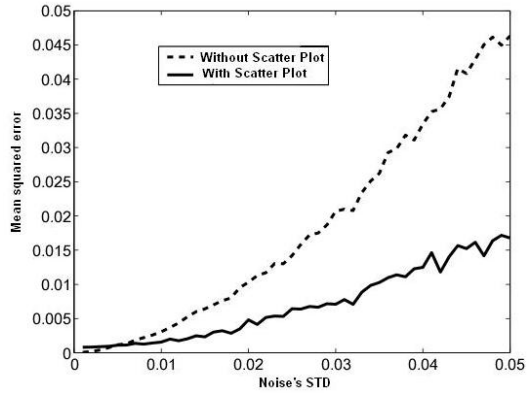


Figure 7 – Mean square error on the estimation of the zenith θ as a function of the noise variance.

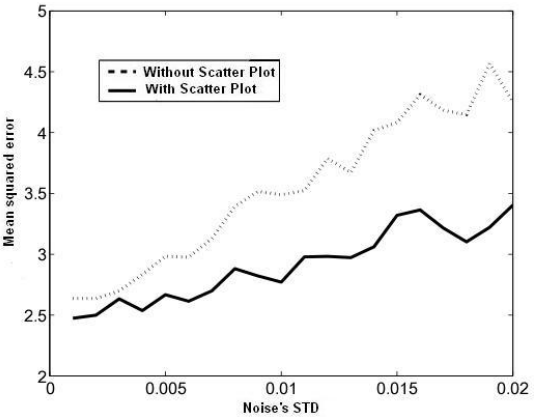


(a)

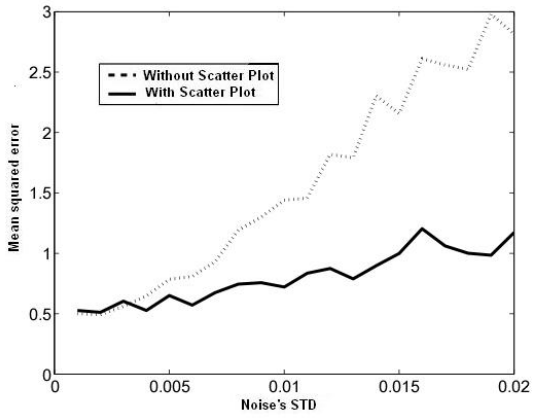


(b)

Figure 8 – Mean square error on surface reconstruction. (a) corresponds to the Wei and Klette method, (b) corresponds to the shapelets method.

## REFERENCES

[1] B. Aiazzi, L. Alparone, A. Barducci, S. Baronti, and I. Pippi. "Estimating noise and information of multispectral imagery", *Society of Photo Optical Instrumentation Engineers*, 2002.

[2] M. Born and E. Wolf. *Principles of optics*. Pergamon Press, New-York, sixth edition, 1983.

[3] B. K. P. Horn. *Robot vision*. MIT Press, 1986.

[4] S. Huard. *Polarisation de la lumière*. Masson, 1994.

[5] K. Koshikawa, "A polarimertric approach to shape understanding of glossy objects", in Proc. of the International Joint Conference on Artificial Intelligence 1979, Tokyo, Japan, August 1979, pp. 493-495.

[6] K. Koshikawa and Y. Shirai. "A model-based recognition of glossy objects using their polarimetric properties", *Advances robotics* vol.2, pp. 137-147, 1987.

[7] P. Kovesi, "Shapelets correlated with surfaces normals produce surfaces", in 10th IEEE International Conference on Computer Vision 2005, Beijing, China, October 17-20. 2006, pp. 994-1001.

[8] D. Miyazaki, M. Kagesawa, and K. Ikeuchi. "Transparent surface modelling from a pair of polarization images", *IEEE Transactions on Pattern Analysis and Machine Intelligence*, vol.26-1, pp. 920-932, 2004.

[9] D. Miyazaki, M. Saito, Y. Sato, and K. Ikeuchi. "Determining surface orientations of transparent objects based on polarization degrees in visible and infrared wavelengths", *J. Opt. Soc. Am A*, Vol.19, pp. 687-694, 2002.

[10] T. Wei and R. Klette, "Depth recovery from noisy gradient vector fields using regularization", in 10th International Conference on Computer Analysis of Image and Patterns 2003, Groningen, The Netherlands, August 25-27. 2003, pp. 116-123.

[11] L.B. Wolff, "Surface orientation from two camera stereo with polarizers". in Proceedings of Optics, Illumination, and Image Sensing for Machin Vision IV 1989, Philadelphia, Pennsylvania, November 1989, pp. 287-297.

[13] L.B. Wolff and T. E. Boult., "Constraining object features using a polarization reflectance model", *IEEE Transactions on Pattern Analysis and Machine Intelligence*, vol. 13, pp. 635-657, 1991.